Atomic Layer Deposition of Nanostructured TiO_2 Photocatalysts via Template Approach

Marianna Kemell,* Viljami Pore, Jere Tupala, Mikko Ritala, and Markku Leskelä

Laboratory of Inorganic Chemistry, Department of Chemistry, University of Helsinki, Helsinki FI-00014, Finland

Received October 29, 2006. Revised Manuscript Received January 26, 2007

Two kinds of TiO_2 nanostructures, i.e., TiO_2-coated alumina membranes and TiO_2-coated Ni nanowires, were prepared by combining different kinds of porous alumina, template-directed electrodeposition and atomic layer deposition. The photocatalytic activities of the nanostructures were tested with methylene blue degradation under UV illumination. All structures showed photocatalytic activity, and the efficiency of the photocatalytic performance was found to be a strong function of the dimensions of the nanostructure.

Introduction

TiO_2 nanotubes and nanowires have a broad range of applications in several areas such as (photo)catalysis,[1,2] photovoltaics,[2] and sensing.[2] Common routes to TiO_2 nanotubes and nanowires include hydrothermal synthesis,[3] electrospinning,[4] and anodization of Ti foils or thin films.[2,5,6] An interesting approach is template-assisted preparation[7] where an existing nanostructure is utilized as a scaffold for the formation of TiO_2 nanotubes or nanowires. Porous alumina[7,8] and track-etched polymer membranes[7,9] are among the most popular templates, but carbon nanotubes,[10] inorganic nanowires,[10,11] and natural fibers[12,13] have been used as well. The advantage of using regularly structured templates such as porous alumina, which consists of straight cylindrical pores with approximately uniform diameters, is that they yield dense, regular arrays of vertical nanotubes and nanowires.

Liquid-phase deposition methods such as electrodeposition,[14,15] sol−gel,[16,17] and hydrolysis of TiF_4[18] or $TiCl_4$[19] are the most popular methods used in template-assisted preparation of TiO_2 nanotubes and nanowires. Thermal decomposition of $Ti(O^iPr)_4$ in the pores of an alumina template has been used as well.[20] In contrast to liquid-phase methods, only few gas-phase methods appear to be suitable for template-assisted preparation of nanotubes and nanowires. As a result of its self-limiting growth mechanism, atomic layer deposition (ALD)[21,22] seems the most promising among gas-phase methods. ALD is a chemical thin film deposition method that can be used to deposit a variety of materials (oxides, metals, sulfides, nitrides, etc.). The self-limiting growth is achieved by pulsing the precursor vapors in the reaction chamber alternately. Each precursor pulse is followed by a purging period which removes the excess precursor molecules and gaseous byproducts from the gas phase and leaves only a saturated (sub)monolayer of the precursor on the substrate surface. Thus the film growth occurs via alternate saturative surface reactions. This unique growth mechanism allows the deposition of high-quality thin films with uniform compositions and thicknesses also on templates with challenging morphologies. Xiong et al.,[23] for example, have successfully used ALD for surface modification of porous alumina membranes. Our group, in turn, has demonstrated the suitability of ALD in preparing photocatalytically active high surface area TiO_2/cellulose composites.[13,24]

* To whom correspondence should be addressed. E-mail: marianna.kemell@helsinki.fi.

(1) Hashimoto, K.; Irie, H.; Fujishima, A. *Jpn. J. Appl. Phys.* **2005**, *44*, 8269.
(2) Mor, G. K.; Varghese, O. K.; Paulose, M.; Shankar, K.; Grimes, C. A. *Sol. Energy Mater. Sol. Cells* **2006**, *90*, 2011.
(3) Bavykin, D. V.; Parmon, V. N.; Lapkin, A. A.; Walsh, F. C. *J. Mater. Chem.* **2004**, *14*, 3370.
(4) Li, D.; Xia, Y. *Nano Lett.* **2003**, *3*, 555.
(5) Zwilling, V.; Darque-Ceretti, E.; Boutry-Forveille, A.; David, D.; Perrin, M. Y.; Aucouturier, M. *Surf. Interface Anal.* **1999**, *27*, 629.
(6) Macak, J. M.; Tsuchiya, H.; Taveira, L.; Aldabergerova, S.; Schmuki, P. *Angew. Chem., Int. Ed.* **2005**, *44*, 7463.
(7) Hulteen, J. C.; Martin, C. R. *J. Mater. Chem.* **1997**, *7*, 1075.
(8) Sander, M. S.; Côté, M. J.; Gu, W.; Kile, B. M.; Tripp, C. P. *Adv. Mater.* **2004**, *16*, 2052.
(9) Shin, H.; Jeong, D.-K.; Lee, J.; Sung, M. M.; Kim, J. *Adv. Mater.* **2004**, *16*, 1197.
(10) Gomathi, A.; Vivekchand, S. R. C.; Govindaraj, A.; Rao, C. N. R. *Adv. Mater.* **2005**, *17*, 2757.
(11) Leskelä, M.; Kemell, M.; Kukli, K.; Pore, V.; Santala, E.; Ritala, M.; Lu, J. *Mater. Sci. Eng. C* **2006**, in press.
(12) Huang, J.; Kunitake, T. *J. Am. Chem. Soc.* **2003**, *125*, 11834.
(13) Kemell, M.; Pore, V.; Ritala, M.; Leskelä, M.; Lindén, M. *J. Am. Chem. Soc.* **2005**, *127*, 14178.
(14) Hoyer, P. *Langmuir* **1996**, *12*, 1411.
(15) Liu, S.; Huang, K. *Sol. Energy Mater. Sol. Cells* **2005**, *85*, 125.
(16) Lakshmi, B. B.; Dorhout, P. K.; Martin, C. R. *Chem. Mater.* **1997**, *9*, 857.
(17) Chu, S.-Z.; Wada, K.; Inoue, S.; Todoroki, S.-i. *Chem. Mater.* **2002**, *14*, 266.
(18) Imai, H.; Takei, Y.; Shimizu, K.; Matsuda, M.; Hirashima, H. *J. Mater. Chem.* **1999**, *9*, 2971.
(19) Park, I.-S.; Jang, S.-R.; Hong, J. S.; Vittal, R.; Kim, K.-J. *Chem. Mater.* **2003**, *15*, 4633.
(20) Michailowski, A.; AlMawlwai, D.; Cheng, G. S.; Moskovits, M. *Chem. Phys. Lett.* **2001**, *349*, 1.
(21) Ritala M.; Leskelä, M. In *Handbook of Thin Film Materials*; Nalwa, H. S., Ed.; Academic Press: San Diego, CA, 2002; Vol. 1, pp 103−159.
(22) Leskelä, M.; Ritala, M. *Angew. Chem., Int. Ed.* **2003**, *42*, 5548.
(23) Xiong, G.; Elam, J. W.; Feng, H.; Han, C. Y.; Wang, H.-H.; Iton, L. E.; Curtiss, L. A.; Pellin, M. J.; Kung, M.; Kung, H.; Stair, P. C. *J. Phys. Chem. B* **2005**, *109*, 14059.
(24) Kemell, M.; Pore, V.; Ritala, M.; Leskelä, M. *Chem. Vap. Deposition* **2006**, *12*, 419.

10.1021/cm062576e CCC: $37.00
Published on Web 02/28/2007

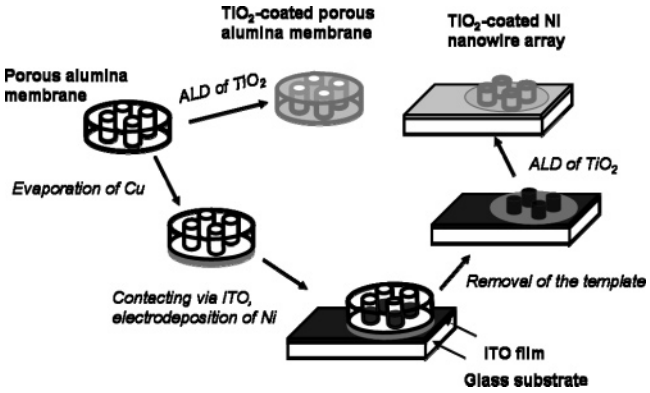

Figure 1. Preparation of the TiO_2 nanostructures starting from porous alumina templates.

Crystallinity is crucial in most applications of TiO_2: anatase is preferred for photocatalysis and photovoltaics, and rutile is preferred for gas sensors.[2] As compared to most liquid-phase methods, one of the advantages of ALD is that it allows the deposition of crystalline TiO_2 films and hence obviates the need for postdeposition annealing. However, in most studies where ALD has been used for the template-assisted preparation of TiO_2 nanotubes, the films have been deposited at such low temperatures that the as-deposited nanotubes have been amorphous.[8,9] Even though the nanotubes crystallized upon annealing,[8] these ALD-grown TiO_2 nanotubes were not tested for photocatalytic activity.

In the current study we compare two ways to prepare photocatalytically active TiO_2 nanostructures via template-directed deposition using either porous alumina or its inverse replica. In both approaches we utilize ALD to deposit anatase TiO_2 thin films on the high aspect ratio templates. The preparation sequences of the TiO_2-coated nanostructures are presented in Figure 1. These are by no means limited to the materials used in this study: the great variety of materials that can be deposited by evaporation, electrodeposition, and ALD enables numerous material combinations for various applications.

Experimental Section

Porous Alumina Membranes. Two types of porous alumina membranes were used as substrates for the TiO_2-coated porous alumina membranes: free-standing commercial Whatman Anodisc membranes (disk diameter 13 mm, thickness 60 μm, pore diameter about 0.2 μm), and self-made, glass-supported thin-film membranes. The thin-film membranes were prepared by anodization of Al thin films (thickness about 700−800 nm; prepared by electron beam evaporation) in 10 wt % H_3PO_4 at 10 °C, 80 V, until transparent.[25,26] To achieve larger pore diameters and thus a higher specific surface area, one sample was subsequently etched chemically in 10 wt % H_3PO_4 at 35 ± 2 °C for 8 min.

Ni Nanowires. First, approximately 20 nm of Cu was evaporated in an oblique angle on one side of a commercial Whatman Anodisc membrane in order to form a conductive back contact for electrodeposition. The Cu-coated face of the Anodisc membrane was then pressed against a conductive ITO-coated glass substrate (ITO = indium tin oxide, In_2O_3:Sn). The ITO-coated glass, in turn, was contacted as the working electrode to an Autolab PGSTAT 20 potentiostat. Ni nanowires were electrodeposited in the pores of the porous alumina template from a solution containing 0.4 M $NiSO_4$ + 0.66 M H_3BO_3 potentiostatically at −1.0 V vs Ag/AgCl. Subsequent dissolution of the Anodisc template in 0.5 M KOH at 40 °C for 1 h exposed the Ni nanowires standing on the ITO-coated substrate (Figure 1).

ALD of TiO_2. TiO_2 films (about 30 nm) were deposited on the nanostructures by ALD in a flow-type F-120 reactor (ASM Microchemistry, Ltd., Finland)[27] according to ref 28 using $Ti(OMe)_4$ and H_2O as the precursors. The deposition temperature was 325 °C. $Ti(OMe)_4$ was evaporated inside the reactor at 130 °C and H_2O in an external reservoir held at room temperature. The precursor vapors were supplied alternately on the nanostructures, and each precursor pulse was followed by a N_2 purge. The reactor was operated under a pressure of about 10 mbar.

To saturate all the reactive surface sites and to give enough time for the diffusion of the precursors and gaseous byproducts in and out of the high aspect ratio structures, longer than normal exposure and purge times were needed. For the porous alumina structures, the exposure and purge times for both precursors were 5 and 10 s, respectively. The growth cycle was repeated 430 times, which resulted in a film thickness of about 31 nm on a planar substrate. In the case of Ni nanowires, the exposure and purge times were 2 and 15 s, respectively, for both precursors. The growth cycle was repeated 500 times.

Characterization. Scanning electron microscopy (SEM) images were acquired with a Hitachi S-4800 field emission scanning electron microscope. Elemental line scans and energy dispersive (EDS) point spectra were measured at 10 keV using an Oxford INCA 350 energy dispersive X-ray microanalysis system connected with the Hitachi S-4800. X-ray diffractograms were measured with a Bruker D8 Advance X-ray diffractometer using Cu Kα radiation. To study the thickness of the TiO_2 film along the pore walls of the Anodisc template, the template was partly dissolved with 0.5 M KOH prior to cross-section field emission scanning electron microscopy (FESEM) imaging.

The photocatalytic activities of the TiO_2 nanostructures were tested with photocatalytic degradation of methylene blue ($C_{16}H_{18}N_3SCl$, MB) in aqueous solution. Samples with a similar footprint area (about 0.2 cm^2) were attached on glass slides with adhesive tape for easier handling. The samples were first immersed in 3 mL of 0.01 mM MB solution and kept in the dark for 1 h to adsorb MB on the sample surface. After this initial adsorption, the irradiation was started. The test was carried out in UV transparent disposable cuvettes, and the irradiation was accomplished through the cuvette windows with a 18 W Sylvania Blacklight Blue UV lamp (peak maximum at 365 nm, intensity ~1.5 mW/cm^2). The concentration of MB in the solution was followed by UV−vis spectroscopy. For comparison, a degradation test with a planar TiO_2 film and a dark test with a TiO_2-coated Anodisc membrane were also conducted.

Results and Discussion

Figure 2a,b shows FESEM images of glass-supported TiO_2-coated porous alumina thin-film membranes prepared by anodization of glass-supported Al thin films. Comparison between parts a and b of Figure 2 clearly shows that the structure in part b is much more open because of the larger

(25) Kemell, M.; Färm, E.; Leskelä, M.; Ritala, M. *Phys. Status Solidi A* **2006**, *203*, 1453.
(26) Miney, P. G.; Colavita, P. E.; Schiza, M. V.; Priore, R. J.; Haibach, F. G.; Myrick, M. *Electrochem. Solid-State Lett.* **2003**, *6*, B42.
(27) Suntola, T. *Thin Solid Films* **1992**, *216*, 84.
(28) Pore, V.; Rahtu, A.; Leskelä, M.; Ritala, M.; Sajavaara, T.; Keinonen, J. *Chem. Vap. Deposition* **2004**, *10*, 143.

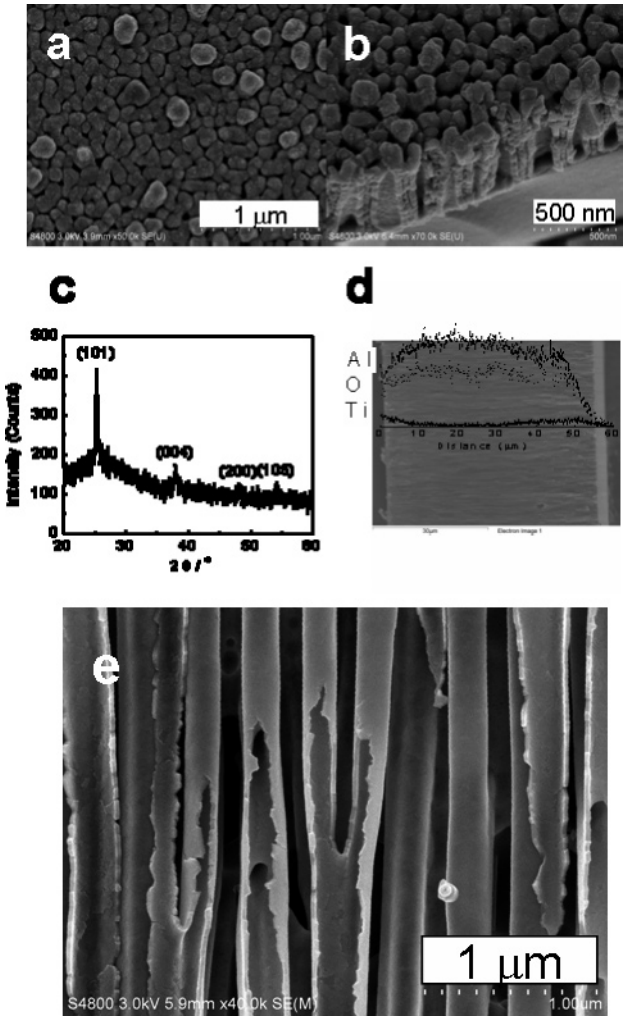

Figure 2. (a, b) FESEM images of TiO_2-coated glass-supported thin-film membranes. (a) Top view of a membrane with small pore diameters, (b) oblique view, showing both surface and cross section of a membrane with larger pore diameters achieved by chemical etching prior to the deposition of TiO_2, (c) X-ray diffractogram of the sample shown in part b, (d) cross-sectional view and corresponding elemental line scans of a TiO_2-coated Anodisc membrane, and (e) FESEM image of TiO_2 nanotubes formed by partly dissolving the Anodisc template.

pore diameter achieved by chemical etching prior to the deposition of TiO_2. The X-ray diffractogram in Figure 2c, measured of the sample shown in Figure 2b, verifies the presence of anatase TiO_2.[29] Figure 2d shows a cross-section FESEM image of a TiO_2-coated Anodisc template and corresponding elemental line scans for Al, O, and Ti, measured along the cross section. It is evident from Figure 2d that Ti is present everywhere, but its distribution is not uniform along the cross section: more Ti is seen near the top and bottom surfaces than close to the center of the template. The presence of Ti in the center of the template was confirmed also with point EDS measurements (not shown). Cross-sectional FESEM images revealed that the thickness of the TiO_2 film was about 30 nm near the top and bottom surfaces (see Figure 2e) and decreased toward the center of the template. Film thickness near the center of the template was too low (below 10 nm) for unambiguous thickness determination. Thus the thickness of the TiO_2 film is not constant along the cross section, which can be attributed to insufficient precursor doses or purging. In the flow-type reactor used in this study, the precursor vapors flow over the substrate, and their transport in and out of the pores by diffusion takes time. Therefore, longer pulse and purge times would probably improve the uniformity. On the other hand, a modified reactor,[30] where the precursor vapors are forced to flow through the pores of the template, would allow more uniform coating with similar pulse and purge times as those used here. Perfect uniformity is not critical for photocatalysis, however.

For comparison, Sander et al.[8] formed TiO_2 nanotubes in porous alumina templates by ALD at 105 °C using $TiCl_4$ and H_2O as the precursors. The templates were made by anodization of 0.2−1.5 μm thick Al films on Si substrates and had average pore spacings of 60−100 nm. The as-deposited nanotubes were amorphous but became crystalline with the anatase structure after annealing at 500 °C for 2 h. Instead of inert gas purging, the reactor was evacuated to 10^{-5} Torr after each precursor pulse. The resulting growth rate, about 0.18 nm/cycle, was higher than usually observed for ALD growth from $TiCl_4$ and H_2O at those temperatures on flat substrates, 0.045−0.061 nm/cycle.[31,32] This suggests the presence of a small CVD component, presumably due to insufficient evacuation between the precursor pulses.[8] The templates of Shin et al.,[9] in turn, were 12 μm thick polycarbonate membranes with pore sizes between 50 and 200 nm. The nanotubes were prepared at 140 °C using Ti-(O^iPr)$_4$ and H_2O as the precursors. The growth rate inside the pores was about 0.05−0.06 nm/cycle, again somewhat higher than the 0.04 nm/cycle observed on flat substrates at the same temperature. It must be noted, however, that the templates used in these studies[8,9] were thinner and thus less demanding to coat than the 60 μm thick Anodisc membrane. Thus the surfaces could be saturated with smaller precursor doses, and also the diffusion in and out of the pores took considerably less time.

The X-ray diffractogram in Figure 3a reveals that the Ni nanowires deposited in the porous alumina template had a face-centered cubic (fcc) structure.[33] This is in agreement with previous observations reported in the literature.[34,35] Figure 3b,c shows FESEM images of an electrodeposited Ni nanowire array after dissolution of the Anodisc template. The length of the Ni nanowires (about 12 μm) seems homogeneous over large areas. It is, however, clearly visible that the nanowires have "bundled" together. The bundling phenomenon is visible also in Figure 4 for a TiO_2-coated Ni nanowire array. This "bundling" originates from the removal of the supporting alumina template and has been observed frequently.[9,15,36]

(29) International Centre for Diffraction Data (ICDD), Card 21-1272.

(30) Ritala, M.; Kemell, M.; Lautala, M.; Niskanen, A.; Leskelä, M.; Lindfors, S. G. *Chem. Vap. Deposition* **2006**, *12*, 655.
(31) Aarik, J.; Karlis, J.; Mändar, H.; Uustare, T.; Sammelselg, V. *Appl. Surf. Sci.* **2001**, *181*, 339.
(32) Kemell, M.; et al. Manuscript in preparation.
(33) International Centre for Diffraction Data (ICDD), Card 4-850.
(34) Chu, S.-Z.; Wada, K.; Inoue, S.; Todoroki, S. *Chem. Mater.* **2002**, *14*, 4595.
(35) Rahman, I. Z.; Razeeb, K. M.; Rahman, M. A.; Kamruzzaman, Md. *J. Magn. Magn. Mater.* **2003**, *262*, 166.
(36) Pan, H.; Chen, W.; Feng, Y. P.; Ji, W.; Lin, J. *Appl. Phys. Lett.* **2006**, *88*, 223106.

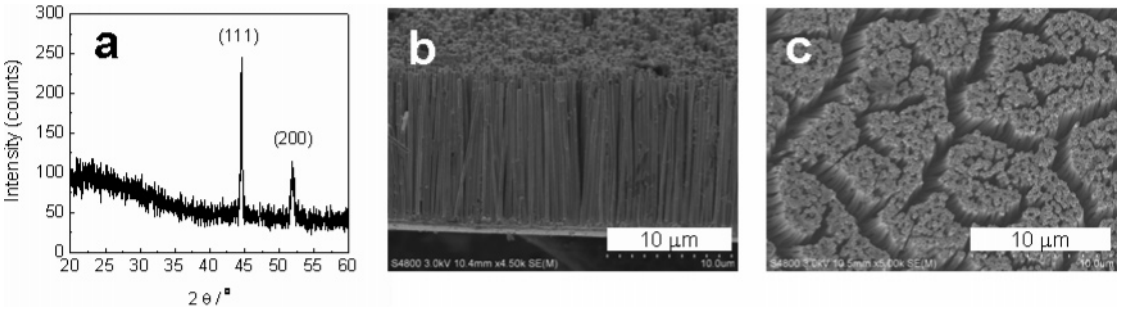

Figure 3. (a) X-ray diffractogram of an electrodeposited Ni nanowire array in the Anodisc and (b, c) FESEM images of electrodeposited Ni nanowire arrays after dissolution of the Anodisc template.

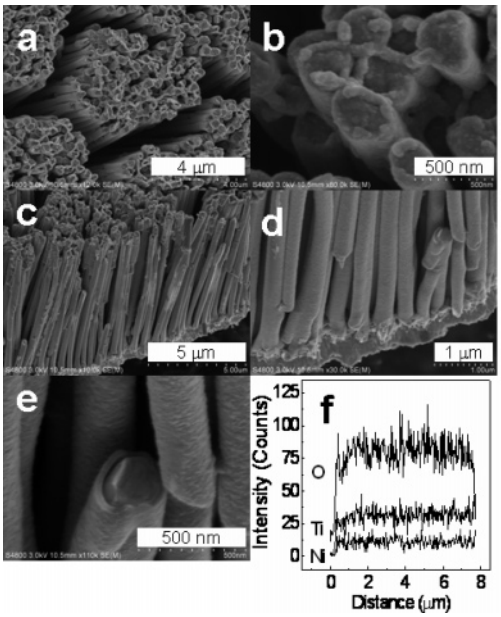

Figure 4. (a−e) FESEM images of a TiO_2-coated Ni nanowire array and (f) elemental line scans for O, Ti, and Ni, measured along a cross section similar to that in part c.

Figure 4 shows FESEM images and elemental line scans acquired from the TiO_2-coated Ni nanowire array. A broken nanowire in Figure 4e reveals a cross section of the TiO_2 film. The film thickness can be seen to be about 30 nm. The elemental line scan in Figure 4f, measured along a cross section, shows quite a homogeneous Ti distribution, indicating a uniform film thickness. Therefore the exposure and purge times used here seemed to be enough for forming a TiO_2 film with uniform thickness. It must be noted that the Ni nanowire structure is shallower (about 8 μm) and thus less demanding than the 60 μm thick Anodisc template. X-ray diffractograms of the TiO_2-coated Ni nanowire arrays (not shown here) showed, in addition to the reflections of fcc Ni, a very weak (101) reflection of anatase TiO_2.[29] This may indicate an effect of the growth surface on the crystallinity: it is possible that the TiO_2 films deposited on Ni have lower crystallinity than the TiO_2 films on the porous alumina.

In addition to photocatalysis, these kinds of TiO_2-coated metal nanowire arrays are interesting as high surface area photoelectrocatalysts or as electrodes in dye-sensitized solar cells.[7] As a result of its high conductivity, a metallic nanowire can evidently carry current in a much more efficient manner than the assembly of semiconducting TiO_2 particles that are commonly used.

Another application area for these arrays could be in nanoimprint lithography (NIL). Earlier, porous alumina templates have been used for preparing aluminum/alumina composites[37] and PMMA rods[38] as molds for NIL. As compared to these approaches,[37,38] a great advantage of a coated metal nanowire array is that it enables easier and more accurate fine-tuning of the dimensions: The length of the nanowires can be adjusted by the duration of electrodeposition and diameter by the coating thickness. Further applications for the coated metal nanowires may be found in optics, for example. Pan et al.[36] studied recently the optical limiting properties of metal nanowires. Modification of the metal nanowires by various coatings is a tempting possibility since it may lead to new optical properties. The coated metal nanowire arrays may also show interesting electrowetting behavior, analogously to what was observed recently for coated carbon nanofibers by Dhindsa et al.[39] As a result of the broad range of materials that can be prepared by ALD, one can choose quite freely the coating material that has the desired (mechanical, electrical, optical, etc.) properties for the application under study. This naturally gives almost unlimited possibilities for the fabrication of various nanostructures.

Photocatalytic TiO_2 has the ability to completely mineralize various organic compounds when subjected to more energetic irradiation than its band gap of approximately 3.2 eV. Various active oxygen species, such as O_2^-, $^{\bullet}OH$, $HO_2^{\bullet}$, and $O^{\bullet}$, are produced on the surface of TiO_2 by photogenerated electrons and holes.[1] Photocatalytic degradation of MB dye has been widely studied, and it is frequently used in the testing of photocatalytic materials. The degradation mechanism has been clarified, and MB was shown to mineralize into CO_2, NH_4^+, NO_3^-, and SO_4^{2-} by photocatalytic TiO_2 under UV irradiation.[40−43]

Figure 5 shows the results on photocatalytic degradation of MB under UV illumination by the TiO_2-coated nano-

(37) Lee, P.-S.; Lee, O.-J.; Hwang, S.-K.; Jung, S.-H.; Jee, S. E.; Lee, K.-H. *Chem. Mater.* **2005**, *17*, 6181.
(38) Goh, C.; Coakley, K. M.; McGehee, M. D. *Nano Lett.* **2005**, *5*, 1545.
(39) Dhindsa, M. S.; Smith, N. R.; Heikenfeld, J.; Rack, P. D.; Fowlkes, J. D.; Doktycz, M. J.; Melechko, A. V.; Simpson, M. L. *Langmuir* **2006**, *22*, 9030.
(40) Houas, A.; Lachheb, H.; Ksibi, M; Elaloui, E.; Guillard, C.; Herrmann, J.-M. *Appl. Catal., B* **2001**, *31*, 145.
(41) Zhang, T.; Oyama, T.; Horikoshi, S.; Hidaka, H.; Zhao, J.; Serpone, N. *Sol. Energy Mater. Sol. Cells* **2002**, *73*, 287.
(42) Lakshmi, S.; Renganathan, R.; Fujita, S. *J. Photochem. Photobiol., A* **1995**, *88*, 163.
(43) Gnaser, H.; Savina, M. R.; Calaway, W. F.; Tripa, C. E.; Veryovkin, I. V.; Pellin, M. J. *Int. J. Mass Spectrom.* **2005**, *245*, 61.

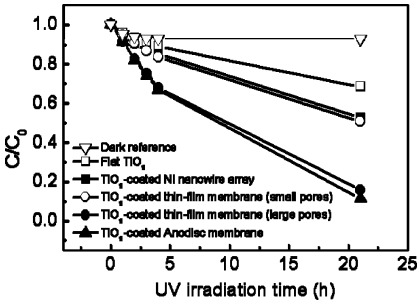

Figure 5. Decrease of MB concentration (C) upon photocatalytic decomposition with the various TiO_2-coated nanostructures. The results for a flat TiO_2 film and the dark reference are also shown for comparison. C_0 is the initial MB concentration.

structures prepared in this work. All the structures were photocatalytically active and showed higher activities than the planar reference sample. The highest activity was observed with the TiO_2-coated Anodisc membrane, but the glass-supported thin-film membrane with larger pore diameters (Figure 2b) showed nearly equal activity despite its much smaller surface area. This is an indication of incomplete utilization of the high surface area of the Anodisc template; it is possible that the deep high aspect ratio structure does not allow for efficient diffusion of the MB dye and its degradation products in and out of the pores. Insufficient penetration of the light all the way to the bottom of the pores is another possible explanation. Anyhow, the high activity of the TiO_2-coated Anodisc template may make it suitable as a photocatalytic filter for water or air purification, for example.

The TiO_2-coated Ni-nanowire sample was also photocatalytically active, but its activity was lower, comparable to that of the glass-supported thin-film membrane with smaller pore diameters (Figure 2a). Analogously to the Anodisc case, this can be explained by the very sheltered structure which may hinder both penetration of light and diffusion of solution species. An additional explanation arises from the possibly lower crystallinity of the TiO_2 film in this structure as compared to the other structures: lower crystallinity leads to lower photocatalytic activity.

When a high surface area sample is immersed in MB solution, the MB concentration starts to decrease because it gets adsorbed on the sample surface. This should be kept in mind when conducting photocatalytic degradation experiments in solution. Control experiments in the dark but under otherwise identical conditions are frequently conducted to see how much adsorption alone contributes to the concentration decrease. In the absence of UV illumination, complete adsorption of MB on the TiO_2-coated Anodisc membrane, that is, the one with the highest surface area, is reached after a few hours (see the uppermost curve in Figure 5). Thus the effect of adsorption alone is negligible, and the decrease of the MB concentration upon illumination is concluded to result from photocatalytic degradation.

TiO_2-coated Ni nanowire arrays with more open structures would be achieved by using templates with narrower pores and thicker pore walls. These kinds of templates can be prepared by anodization of Al or by narrowing the pores of an Anodisc template by depositing, for example, Al_2O_3 by ALD[44] prior to the electrodeposition of the metal nanowire array. Exploration and development of these possibilities will be a subject of a further study.

Conclusion

TiO_2-coated membranes were prepared by coating porous alumina with ALD and TiO_2-coated Ni nanowire arrays by combining template-directed electrodeposition into porous alumina and ALD. The effect of the increased surface area was clearly visible in the photocatalytic activity results: all nanostructures showed higher photocatalytic activities than the flat reference sample. The highest activities were observed with TiO_2-coated alumina membranes with relatively open structures. Lower activities were measured for the more sheltered structures such as the TiO_2-coated Ni nanowire array and the TiO_2-coated alumina membrane with narrower pores. The structures may be useful as high surface area photocatalysts; particularly, the TiO_2-coated alumina membrane could be used as a water or air purification filter. The TiO_2-coated Ni nanowire arrays, in turn, may find additional applications in photoelectrocatalysis, NIL, and optics, for example. One of the advantages of ALD is the broad range of materials that can be deposited, enabling thus the fabrication of various functional nanostructures with tailored electrical, mechanical, or other properties.

Acknowledgment. The authors thank the Academy of Finland (Project Nos. 201564 and 209739) and the Finnish National Technology Agency (TEKES, Technology program Clean Surfaces 2002−2006) for financial support.

CM062576E

(44) Ott, A. W.; Klaus, J. W.; Johnson, J. M.; George, S. M.; McCarley, K. C.; Way, J. D. *Chem. Mater.* **1997**, *9*, 707.